metals

MDPI

Article

The Relationship between Nil-Strength Temperature, Zero Strength Temperature and Solidus Temperature of Carbon Steels

Petr Kawulok [1,*], Ivo Schindler [1], Bedřich Smetana [1], Ján Moravec [2], Andrea Mertová [1], Ľubomíra Drozdová [1], Rostislav Kawulok [1], Petr Opěla [1] and Stanislav Rusz [1]

1 Faculty of Materials Science and Technology, VSB–Technical University of Ostrava, 17. listopadu 2172/15, 70800 Ostrava-Poruba, Czech Republic; ivo.schindler@vsb.cz (I.S.); bedrich.smetana@vsb.cz (B.S.); andrea.mertova.st@vsb.cz (A.M.); lubomira.drozdova@vsb.cz (Ľ.D.); rostislav.kawulok@vsb.cz (R.K.); petr.opela@vsb.cz (P.O.); stanislav.rusz2@vsb.cz (S.R.)

2 Faculty of Mechanical Engineering, University of Žilina, Univerzitná 8215/1, 01026 Žilina, Slovakia; jan.moravec@fstroj.uniza.sk

* Correspondence: petr.kawulok@vsb.cz; Tel.: +420-597-324-309

Received: 26 February 2020; Accepted: 18 March 2020; Published: 20 March 2020

Abstract: The nil-strength temperature, zero strength temperature and solidus temperature are significant parameters with respect to the processes of melting, casting and welding steels. With the use of physical tests performed on the universal plastometer Gleeble 3800 and calculations in the IDS software, the nil-strength temperatures, zero strength temperatures and solidus temperatures of nine non-alloy carbon steels have been determined. Apart from that, solidus temperatures were also calculated by the use of four equations expressing a mathematical relation of this temperature to the chemical composition of the investigated steels. The nil-strength and zero strength temperatures and the solidus temperatures decreased with increasing carbon content in the investigated steels. Much higher content of sulfur in free-cutting steel resulted in a decrease of all the temperatures investigated. The zero strength temperatures determined by calculation in the IDS software during solidification were approximately 43–85 °C higher than the nil-strength temperatures determined experimentally during heating of the investigated steels. The linear dependence of experimentally measured nil-strength temperature on the calculated zero strength temperature for the investigated steels was determined. Based on regression analyses, there were determined mathematical relations which described with high accuracy a linear dependence of the nil-strength and zero strength temperatures on the solidus temperature of the investigated steels.

Keywords: carbon steels; nil-strength temperature; zero strength temperature; solidus temperature

1. Introduction

Temperature is a significant parameter, not only for processes of melting, casting and hot forming, but also, for example, for steel welding. For the sake of optimizing of the existing processes of steel manufacturing and processing, it is important to know phase transformation temperatures, or temperatures at which steel loses its plasticity or strength [1–6].

Knowing the liquidus and solidus temperatures is one of the most important factors for processes related to steel melting and casting. These temperatures are critical parameters for the correct setting of physical or numerical models and are equally important for the optimal setting of real processes of steel melting and casting. The correct determination of these temperatures significantly influences the quality and properties of semi-finished cast products (ingots or continuously cast blanks) [7–10].

The nil-strength temperature *NST* (°C) is obtained during the research of brittleness and sensitivity to steel cracking (of other metallic materials) at very high temperatures. It is a very important parameter for welding and for the selection of upper forming temperatures. Technical literature, as regards to material welding and forming processes, specifies the nil-strength temperature as the temperature at which the steel loses, during heating, all its strength due to the melting of grain boundaries. At this temperature, which is lower than the solidus temperature, steel is not able to bear any loading. [5,6,11–13].

In the technical literature related to the issue of material solidification during its casting, in general, the zero strength temperature *ZST* (°C), at which the loading forces can be transferred perpendicularly to the direction of material solidification, can be found. This temperature should correspond to a 65–80% portion of the steel in the solid state and is, thus, higher than the solidus temperature [14–16]. The definitions of the nil-strength temperature and zero strength temperature are thus different.

It is important not to replace the nil-strength temperature or zero strength temperature with the nil-ductility temperature *NDT* (°C). The nil-ductility temperature during tensile tests corresponds to the temperature at which the steel ductility equals to zero (achieving 100% of the material's brittleness). Knowing the nil-strength temperature of steel is important, especially due to the elimination of the origination of cracks at very high temperatures (for example, during welding or casting), because this temperature, together with a ductility recovery temperature, delimits the high-temperature brittleness range. Within this brittleness temperature range, steel at cooling during solidification is sensitive to segregative cracking due to a local loss of ductility of the grain boundaries [5,6,11,13,17].

Methods of the study of the metallurgical processes are based on knowledge of the thermodynamic properties of the materials during their processing by the given technologies. Important temperatures for steel heating and cooling can be determined mathematically or using simulations in specially developed software products; for example, IDS (version 2.0.0, Laboratory of Metallurgy, Helsinky University of Technology, Helsinky, Finland), Thermo-calc, QTSteel, JMatPro and so on. [18–23]. To calculate the solidus temperature, it is possible to use parametric equations, which are based on the melting temperature of pure iron (usually 1536 °C, according to some data; however, from 1528 to 1539 °C) and include the influences of the elements selected in the steel being invetigated. The determination of the solidus temperature on the basis of the computational equations—compared with the experimental determination—is a simpler, quicker and financially non-demanding method. The validity of each equation is, however, limited by a range of the chemical composition for which the given equation was developed [3,4,24,25].

The second approach is the possibility of using physical simulations or measurements which are performed on sophisticated laboratory devices. The solidus and liquidus temperatures and another transformation temperatures of iron, steel and other alloys can be determined, for example, by the use of differential thermal analysis (DTA), with the help of differential scanning calorimetry (DSC), or with the use of thermal-derivative analysis (TDA) [1,21,26–30]. However, when considering the dimensions and possible chemical and structural inhomogeneity of the analyzed sample, it is very difficult to precisely determine the solidus temperature with the use of the sophisticated DTA and DSC methods [1,7,18,28,31]. Won and Thomas [32] reported that during the solidification processes, an important role is also played by microsegregation. The paper [32] also confirmed that the solidus temperature is significantly lowered by the independent increases in either the cooling rate or dendrite arm spacing. The phosphorus and sulfur concentrations have significant effects on the solidus temperature due to their enhanced segregation near the final stage of solidification [32]. In addition, Gryc et al. [1] reported that significant discrepancies between the thermo-analytically measured solidus temperature and the values obtained by the reported formula (up to 42 °C) or the software-based thermodynamic calculations (up to 50 °C) exist.

The nil-strength temperatures of the metal materials can be experimentally determined by the use of relatively simple tests on the universal plastometer Gleeble 3800 (Dynamic Systems Inc., Poestenkill, NY, USA). To enable correct physical determination of the nil-strength temperature, the given laboratory

device must primarily meet two conditions. The specimen has to be heated under control by a low rate (1 to 2 °C·s^{-1}) up to the approaching-melting-point temperature, and the laboratory device has to provide the minimum pre-strained state of the testing specimen and keep it at a constant value (which is problematic due to the thermal expansion). The plastometer Gleeble 3800 meets both presumptions thanks to a special supplemental device [5,11,33].

The main aim of the presented paper was to determine the nil-strength temperatures and zero strength temperatures of selected non-alloy carbon steels and then mathematically describe their dependencies on the solidus temperatures of the investigated steels.

2. Materials and Methods

2.1. Characteristics of the Investigated Steels

For this experiment, nine non-alloy carbon steels have been selected, because they cover a wide range of the carbon content (0.008–0.885 wt.%)—see Table 1—and their chemical compositions are not significantly different. A purposeful exception is represented by a free-cutting steel B with increased content of sulfur (0.311%) and manganese (1.13%). By omitting these excesses, the contents of significant elements fluctuated in the following ranges: 0.14–0.75% Mn; 0.02–0.29% Si; 0.008–0.055% P; 0.006–0.028% S; 0.03–0.27% Cr; and 0.002–0.036% Al. A small quantity of copper and nickel (approximately 0.02%) and other elements (for example, molybdenum, wolfram, vanadium, titanium, and niobium) in thousandths of percent were also identified in the steels.

Table 1. Chemical compositions of the investigated steels in wt.%.

Steel	C	Mn	Si	P	S	Cr	Al	Ni	Cu
A	0.008	0.14	0.020	0.008	0.017	0.04	0.003	0.01	0.01
B	0.087	1.13	0.030	0.055	0.311	0.03	0.003	0.03	0.03
C	0.098	0.38	0.065	0.009	0.020	0.05	0.036	0.02	0.06
D	0.160	0.37	0.055	0.017	0.006	0.06	0.035	0.03	0.04
E	0.384	0.75	0.246	0.018	0.028	0.17	0.026	0.02	0.03
F	0.458	0.71	0.291	0.013	0.023	0.27	0.021	0.03	0.04
G	0.574	0.72	0.251	0.019	0.016	0.07	0.025	0.03	0.04
H	0.733	0.53	0.220	0.009	0.013	0.03	0.002	0.01	0.01
I	0.885	0.67	0.195	0.011	0.013	0.04	0.003	0.02	0.03

2.2. Determination of Nil-Strength Temperature, Zero Strength Temperature and Solidus Temperature

For the determination of the nil-strength temperatures, cylindrical specimens of diameter 6 mm and length 81 mm were prepared from the investigated steels which were supplied in the form of cuttings from continuously cast billets. From these industrially made cast billets (with the cross-sections of 150 × 150 mm), casting crusts of thickness 10 mm wer cut off. Subsequently, square bars (cross-section 10 × 10 mm) were cut longitudinally from the subsurface areas of these cast billets, from which the cylindrical specimens for the plastometer Gleeble 3800 were machined. The central area (with possible segregations) of the cast billets was not used. These cylindrical specimens were clamped into the plastometer Gleeble 3800 between special jaws which were cooled by water. The right jaw (stationary) is firmly fixed to the work chamber of the plastometer; the left jaw (movable) is connected with a pneumatic piston which, during the course of the whole test, acts on the specimen during its heating with the constant tensile force of 80 N (as can be seen in Figure 1). Due to the necessity to use high-temperature heating, the temperature during all tests was measured by platinum thermocouples type R (PtRh13–Pt) which were surface-welded in the centers of the specimens. Electric resistance heating of the specimens was two-stage in the case of this experiment; in the temperature range of 0–1200 °C, the heating rate of 20 °C·s^{-1} was applied, and in the range of 1200–1600 °C the heating rate of 2 °C·s^{-1} was applied. Due to the combination of the very small tensile force of 80 N and the melting of grain boundaries, the specimen was ruptured and the measured temperature suddenly declined.

The experimentally determined nil-strength temperature corresponded to the highest value of the registered temperature at the moment of the loss of material consistency. This test was repeated three times due to the exclusion of the influence of possible non-homogeneities in the investigated steels and also for a statistical assessment. All these tests were carried out under a vacuum of 10^{-3} Pa. These conditions enabled us to correct the physical determination of the nil-strength temperature [5,11,33].

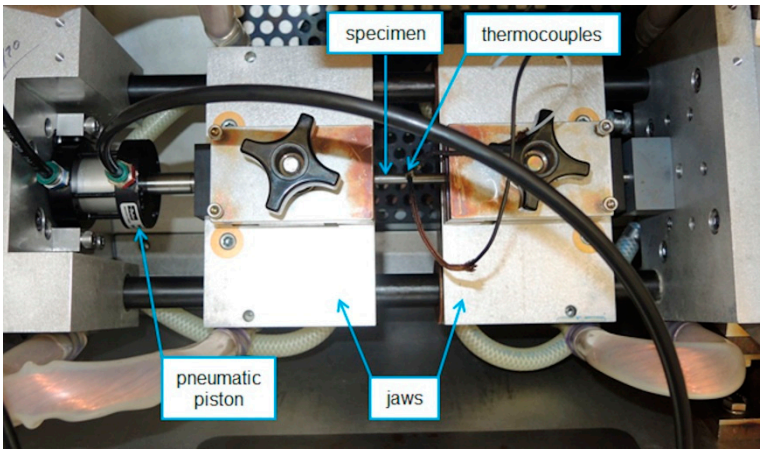

Figure 1. Photograph of a specimen fixed between special jaws with pneumatic pistons for the determination of nil-strength temperature in the plastometer Gleeble 3800.

By using the IDS software, the zero strength temperature and the solidus temperature were determined at the equilibrium conditions of solidification of the investigated steels. The IDS software with a thermodynamic-kinetic model was developed for the simulation of the phase transformations during solidification of low-alloy and anticorrosive steels. For the calculation of phase-transformation temperatures, the IDS software uses thermodynamic equations considering a chemical potential and weight balance, wherein Fick's second law is applied. Depending on the chemical composition of steel and a chosen equilibrium or non-equilibrium state during cooling, the software determines the zero strength temperature, phase transformation temperatures, a portion and composition of the phases for different temperatures and other parameters [34–36].

Based on a literature search, several parametric equations for the calculation of solidus temperature T_S (°C) were found. All these equations express the dependence of the solidus temperature on the chemical composition (in wt.%) of each investigated steel, thereby finding the dependencies on the contents of select elements in the steels. Takeuchi and Brimacombe [25] have used the following equation for the calculation of T_S:

$$T_S = 1536 - 415.5{\cdot}C - 183.9{\cdot}S - 124.5{\cdot}P - 6.8{\cdot}Mn - 12.3{\cdot}Si - 4.1{\cdot}Al - 1.4{\cdot}Cr - 4.3{\cdot}Ni \quad (1)$$

To calculate the T_S temperature, Thomas et al. [4] have used the equation:

$$T_S = 1535 - 200{\cdot}C - 183.9{\cdot}S - 124.5{\cdot}P - 6.8{\cdot}Mn - 12.3{\cdot}Si - 4.1{\cdot}Al - 1.4{\cdot}Cr - 4.3{\cdot}Ni \quad (2)$$

Štětina has used this equation for the the T_S temperature calculation [3]:

$$T_S = 1536 - 251{\cdot}C - 183.9{\cdot}S - 123.4{\cdot}P - 6.8{\cdot}Mn - 12.3{\cdot}Si - 3.6{\cdot}Al - 1.4{\cdot}Cr - 3.3{\cdot}Ni - 3.1{\cdot}Cu \quad (3)$$

Diederichs and Bleck [24] have used the following equation for the T_S temperature calculation:

$$T_S = 1536 - 344{\cdot}C - 183.5{\cdot}S - 124.5{\cdot}P - 6.8{\cdot}Mn - 12.3{\cdot}Si - 4.1{\cdot}Al - 1.4{\cdot}Cr - 4.3{\cdot}Ni \quad (4)$$

The Equations (2) to (4) are, in principle, a modification of Equation (1), which was represented by Takeuchi and Brimacombe [25] already in 1985. The Equations (1) to (4) differ by the coefficients which are primarily applied for the multiplication of the weight content of carbon, and, in some cases also by a slight correction of coefficients applied for the multiplication of the weight content of sulfur (4), phosphorus (3), aluminum (3) or nickel (3). Equation (3) additionally includes the influence of copper on the calculation.

The solidus temperature was not experimentally determined and only parametric equations were used for this purpose. The reason for this was the effort to determine the mathematical relationship that would express a simple dependence of nil-strength temperature and zero strength temperature on the solidus temperature and simultaneously include the influence of the chemical compositions of the investigated steels.

3. Results and Discussion

3.1. Evaluation of the Nil-Strength Temperature and Zero Strength Temperature

The experimentally determined nil-strength temperature corresponded to the highest value of the registered temperature at the moment of loss of material consistency (due to the combination of the action of the tensile force of 80 N and melting of grain boundaries), which was accompanied by the steep decline of the measured temperature (examples of data records are specified in Figure 2). In the case of the steel A (with the lowest content of carbon), during its heating, in spite of the very small action of the tensile force, the testing rods were prolonged, and the resultant nil-strength temperatures were, in this case, burdened by a relatively significant dispersion. During the testing of other investigated steels, the testing rod was not prolonged, but after achieving the nil-strength temperature, brittle fracture occurred.

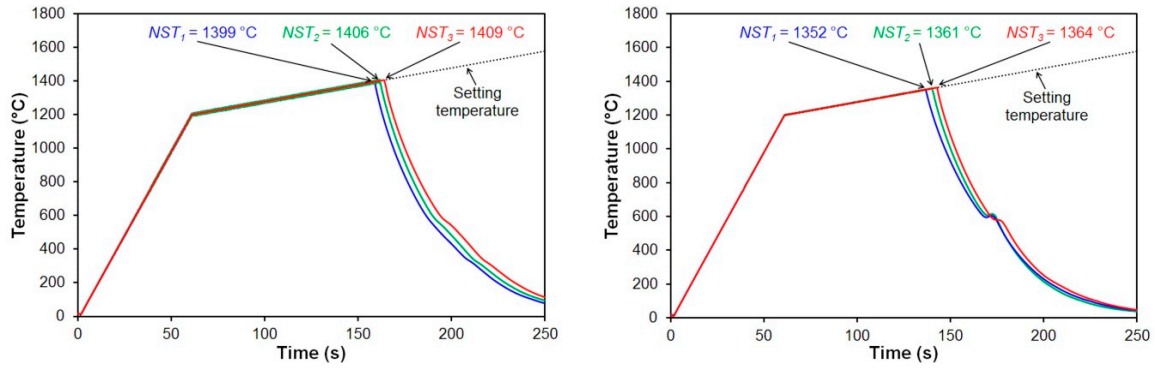

Figure 2. Graphical determination of the nil-strength temperature of the selected investigated steels: (**a**) steel E, (**b**) steel H.

The average values of the measured nil-strength temperatures, *NST* (°C), of the investigated steels and the corresponding standard deviations are presented in Table 2. Table 2 also includes the zero strength temperatures, *ZST* (°C), which were determined in the IDS software via calculations considering the solidification of the investigated carbon steels under equilibrium conditions. The calculated zero strength temperatures of the steels A and B were obtained with the help of the IDS software, even though their chemical compositions—content of carbon in steel A and the content of sulfur and phosphorus in the steel B—were out of the range of the calculation module of this software (from 0.01 to 1.2 wt.% C, to 0.05 wt.% P and S). The zero strength temperatures of the steels A and B determined by the IDS software can, therefore, be burdened by a certain computing error. In Table 2, there is also

specified a difference between the measured nil-strength temperature and calculated zero strength temperature, ΔT (°C), of the investigated steels:

$$\Delta T = ZST - NST \quad (5)$$

Table 2. Determined nil-strength and zero strength temperatures of the investigated steels.

Steel	*NST* (°C)	Standard Deviation (°C)	*ZST* (°C)	Δ*T* (°C)
A	1465	33.3	1526	61
B	1413	3.8	1483	70
C	1444	5.2	1507	63
D	1450	5.4	1493	43
E	1405	4.1	1458	53
F	1387	6.5	1448	61
G	1369	2.3	1433	64
H	1359	4.9	1414	55
I	1306	9.2	1391	85

For all the steels we investigated, the zero strength temperatures calculated by using the IDS software were higher than the experimentally determined nil-strength temperatures. The difference between the *ZST* and *NST* fluctuated from 43 to 85 °C depending on the carbon content of the investigated steels. Based on these results, it appears that the nil-strength temperature determined while heating is not the same as the zero strength temperature determined during solidification of the investigated steels. This fact can be explained by different definitions of nil-strength temperature during the heating of the material [12,17,37] and definition of zero strength temperature during the solidification of the material [14–16]. In both cases, however, the nil-strength and zero strength temperatures decline with the increasing carbon content in the investigated steels, as shown in Figure 3.

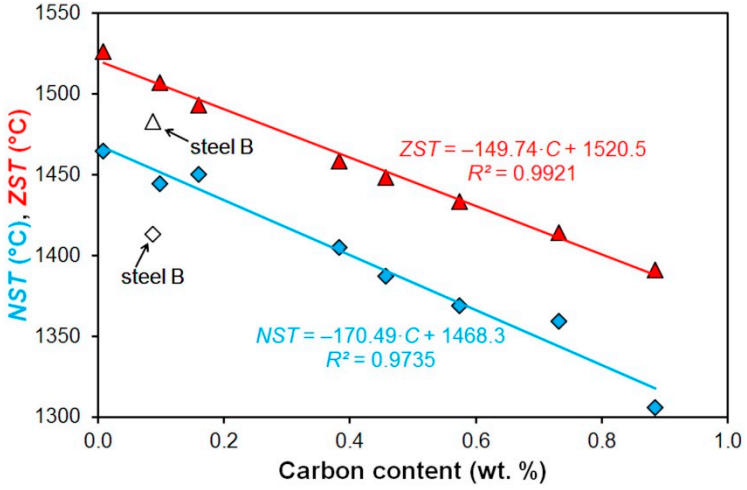

Figure 3. Comparison of the measured nil-strength temperatures and calculated zero-strength temperatures of the investigated steels.

The dependencies of the measured nil-strength temperature and calculated zero strength temperature on the carbon content of the investigated steels (except the free-cutting steel B) can be described with the simple linear equations:

$$NST = -170.49 \cdot C + 1468.3 \quad (6)$$

$$ZST = -149.74 \cdot C + 1520.5 \quad (7)$$

High values of the determination coefficients—(R^2) 0.9735 and 0.9921 for the Equations (6) and (7), respectively—prove the relatively good accuracy. With the help of Equations (6) and (7), it is thus possible to simply predicate the nil-strength temperature during heating and also zero strength temperature during solidification of the carbon non-alloy steels in the range from 0.008 to 0.885 wt.% C.

Using both methods, it was determined that a much higher content of sulfur in the steel B caused a significant decline of the measured nil-strength temperature and calculated zero strength temperature. This finding was surprising, especially in the case of determination of zero strength temperature when using the IDS software. The calculation module range of this software is in the case of sulfur lower by an order of magnitude than the content of sulfur in the steel B. In the case of the plastometric test, the decrease of the nil-strength temperature of the steel B can be influenced by so-called brittleness at glowing heat; this is when steel with a high content of sulfur expresses itself at temperatures above 1200 °C. The reason is the transition of sulfur to low-melting sulfides of FeS or FeS–MnS, which exude on the grain boundaries, and their melting point fluctuates around 1200 °C [38]. This proposition, however, was not verified because plastometrically tested specimens from this steel were not subjected to the SEM analysis.

Based on the results, it was possible to determine the dependence of the experimentally measured nil-strength temperatures on the calculated zero strength temperatures of the investigated steels (as can be seen in Figure 4). This relationship can be described by the simple equation:

$$NST = 1.1097 \cdot ZST - 222.03 \quad (8)$$

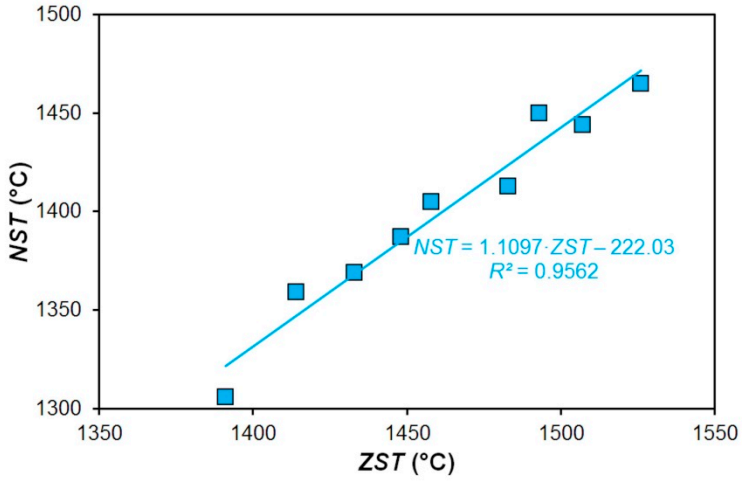

Figure 4. Dependence of the measured nil-strength temperature on the calculated zero strength temperature.

3.2. Evaluation of Solidus Temperature

The solidus temperatures, determined by using Equations (1)–(4), are shown in Table 3. Their mutual comparison is presented in Figure 5. In the case of the low-alloy steel A, the IDS software was not able to determine a solidus temperature because the content of carbon of this steel was out of the range of the calculation module of the IDS software. In the case of the steel B, however, the IDS software has surprisingly generated the solidus temperature even though the content of sulfur and phosphorus was out of the range of the calculation module of the IDS software. The increased content of sulfur in the steel B resulted, similarly to the cases of the nil-strength and zero strength temperatures, in decreasing the solidus temperature in all cases of the computational relations. Based on Figure 5 and Table 3, it is clear that Equations (1) and (4) cannot be applied for the calculation of the solidus temperature for all investigated steels, due to their range of chemical compositions. The solidus temperatures of the middle-carbon and high-carbon steels E–I determined according to Equations (1)

and (4), and compared with the analogical temperatures determined by using Equations (2) and (3) and the IDS software, were significantly lower. The solidus temperatures calculated by using Equations (1) and (4) in comparison with the determined nil-strength and zero strength temperatures of investigated steels were significantly lower too. The Equations (1) and (4) can be used for the determination of the solidus temperature only in the case of a low or middle carbon steels. Very close results for the calculations of the solidus temperature were obtained in the case of using Equations (2) and (3) and in the case wherein calculations were performed in the IDS software.

Table 3. Calculated solidus temperatures of the investigated steels.

Steel	T_S (°C)				
	Equation (1)	Equation (2)	Equation (3)	Equation (4)	Software IDS
A	1527	1528	1529	1528	-
B	1428	1445	1442	1434	1464
C	1487	1507	1503	1494	1477
D	1463	1496	1489	1474	1482
E	1361	1442	1424	1388	1429
F	1331	1429	1406	1364	1411
G	1284	1407	1378	1325	1391
H	1222	1379	1342	1274	1372
I	1157	1347	1303	1221	1347

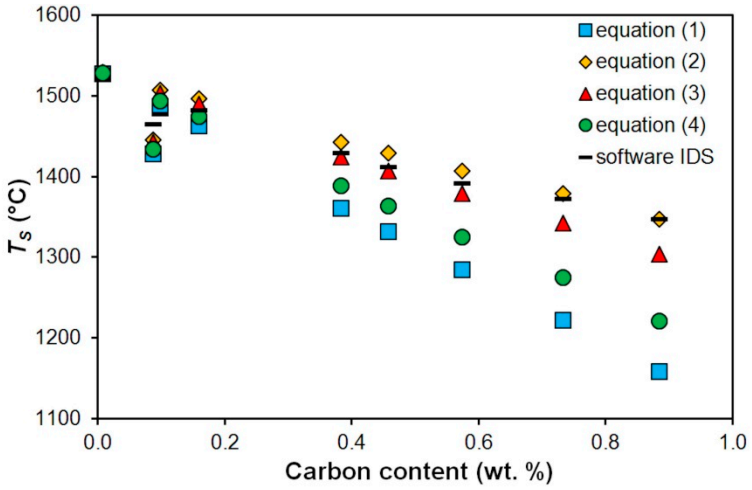

Figure 5. Comparison of the calculated solidus temperatures of the investigated steels.

3.3. The Dependence of the Nil-Strength Temperature and the Zero Strength Temperature on the Solidus Temperature of Investigated Steels

A regression analysis of the relation of the nil-strength and zero strength temperatures with the solidus temperature of the investigated carbon steels has been consequently performed. For these purposes, the solidus temperatures calculated only by using Equations (2) and (3) have been used, because by using these two equations, similar results were achieved. The paper [1] experimentally verified the possibility of the use of Equation (3) for determining the solidus temperatures of steels with a wide range of chemical compositions. The solidus temperatures determined according to the Equations (1) and (4) were excluded from the consequential analyses because they showed the aforementioned inaccuracies already. The solidus temperatures determined with the use of the IDS software were also excluded from these analyses because the calculating module of this software does not use simple parametric equations (expressing an influence of the chemical composition) for the calculation of a solidus temperature, but uses thermodynamic equations, an equality of the chemical potentials, the inter-phase weight of the balance and Fick's second law.

The differences between the experimentally determined nil-strength temperature, calculated zero strength temperature and the solidus temperature (Equations (2) and (3)) of the investigated steels are presented in Table 4. As it is also clear from Table 4, the measured nil-strength temperatures are lower than the solidus temperatures, while calculated zero strength temperatures are almost always higher than the solidus temperatures of the investigated steels. The nil-strength temperature determined experimentally during steel heating corresponds to the moment of grain boundary melting, and should thus be lower than the solidus temperature, which corresponds to the statement in [5,6]. On the contrary, the zero strength temperature determined by calculation in the IDS software, in the case of the low-alloy steels A, C and D, was almost equal with the solidus temperature of the investigated steels. In the case of steels with higher contents of carbon (i.e., from 0.384 wt.%), the difference between the zero strength temperature determined by calculation in the IDS software and the solidus temperature was increasing. It supports the statement in [14,15] that the zero strength temperature determined during solidification of steel should be higher than the solidus temperature because at the moment of its achieving, 20–35% of material should remain in the molten state.

Table 4. Differences between determined nil-strength temperatures, zero strength temperatures and solidus temperatures of the investigated steels.

Steel	$NST - T_S$(2) (°C)	$NST - T_S$(3) (°C)	$ZST - T_S$(2) (°C)	$ZST - T_S$(3) (°C)
A	−63	−64	−2	−3
B	−32	−29	38	41
C	−63	−59	0	4
D	−46	−39	−3	4
E	−37	−19	16	34
F	−42	−19	19	42
G	−38	−9	26	55
H	−20	17	35	72
I	−41	3	44	88
Standard deviation (°C)	13.0	25.3	16.9	29.8

Because of a lower standard deviation in the relation between the measured nil-strength temperatures or calculated zero strength temperatures and solidus temperatures determined according to Equation (2) (as can be seen in Table 4), only this equation was applied for the consequential analysis. Using regression analysis, a linear dependence of the measured nil-strength temperature and calculated zero strength temperature on the solidus temperature of the investigated steels determined according to Equation (2) was determined (as can be seen in Figure 6). These linear dependencies can be described by simple equations that enable easy prediction of the nil-strength temperature and zero strength temperature of non-alloy carbon steels with carbon contents from 0.008 to 0.885 wt.%, including the free-cutting steel B based on knowing the solidus temperature (calculated using Equation (2)):

$$NST = 0.8268 \cdot T_S + 205.98 \quad (9)$$

$$ZST = 0.7283 \cdot T_S + 408.64 \quad (10)$$

High accuracy of the above-mentioned equations is documented by the high values of the determination coefficients, $R^2 = 0.9738$ in the case of the NST and $R^2 = 0.9965$ in the case of the ZST. The main benefit of Equations (9) and (10) is an inclusion of a more significant influence of the chemical composition of steel through the calculation of the solidus temperature (see Equation (2)). Equations (9) and (10), in comparison to Equations (6) and (7), also react to the decline of the nil-strength and zero strength temperatures due to the increased content of sulfur in the free-cutting steel B (as can be seen in Tables 5 and 6). The results obtained from Equations (9) and (10) in comparison with the results obtained from Equations (6) and (7) showed a lower standard deviation of the relative error

of the backward calculation of the nil-strength and zero strength temperature and higher correlation coefficients (as can be seen in Tables 5 and 6).

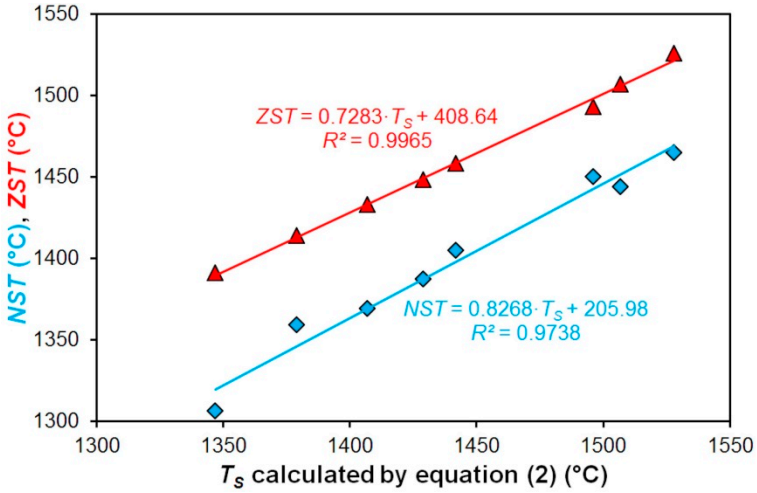

Figure 6. Dependence of the measured nil-strength temperature and the calculated zero strength temperature on the solidus temperature of the investigated steels.

Table 5. Evaluation of accuracy of Equations (6) and (9) intended for the calculation of the nil-strength temperatures of the investigated steels.

Steel	*NST*(exp.) (°C)	*NST*(6) (°C)	*NST*(9) (°C)	*NST*(exp.) − *NST*(6) (%)	*NST*(exp.) − *NST*(9) (%)
A	1465	1467	1469	−0.1	−0.3
B	1413	1453	1401	−2.8	0.8
C	1444	1452	1452	−0.6	−0.6
D	1450	1441	1443	0.6	0.5
E	1405	1403	1398	0.1	0.5
F	1387	1390	1387	−0.2	0
G	1369	1370	1369	−0.1	0
H	1359	1343	1346	1.2	1.0
I	1306	1317	1320	−0.8	−1.1
	Standard deviation (°C)			1.1	0.6
	Correlation coefficient			0.9554	0.9836

Table 6. Evaluation of accuracy of Equations (7) and (10) intended for the calculation of the zero strength temperatures of the investigated steels.

Steel	*ZST*(IDS) (°C)	*ZST*(7) (°C)	*ZST*(10) (°C)	*ZST*(IDS) − *ZST*(7) (%)	*ZST*(IDS) − *ZST*(10) (%)
A	1526	1519	1521	0.5	0.3
B	1483	1507	1461	−1.6	1.5
C	1507	1506	1506	0.1	0.1
D	1493	1497	1498	−0.3	−0.3
E	1458	1463	1459	−0.3	−0.1
F	1448	1452	1449	−0.3	−0.1
G	1433	1435	1433	−0.1	0
H	1414	1411	1413	0.2	0.1
I	1391	1388	1390	0.2	0.1
	Standard deviation (°C)			0.6	0.5
	Correlation coefficient			0.9817	0.9848

In the paper [39], results of similarly focused experiments leading to the determination of the linear dependence between solidus temperature and zero strength temperature of unalloyed steels with 0.003–1.60 wt.% C were published. The difference for these results in comparison to Equations (9)

and (10) is mainly due to the choice of the alloys tested, the fundamentally different methodology of the experiment and the method of determining the solidus temperature. The investigated steels contained a minimized content of other elements (e.g., no more than 0.49% Mn; 0.004% P and 0.004% S). This made it possible to determine the T_S values as equilibrium solidus temperature in Fe-C binary alloys. Alloys characterized in Table 1 are the common carbon steels with up to 1.13% Mn, 0.055% P, 0.311% S (in the case of free-cutting steel) and 0.27% Cr. Their solidus temperatures were not determined experimentally, but by more complex and still more efficient parametric equations. The mathematical determination of T_S values subsequently enables, with high accuracy, a simple prediction of the *NST* and *ZST* values considering the chemical compositions of the investigated steels. Zero strength temperature was determined in [39] on specimens which were in-situ melted, solidified and tensile tested at the specified temperature upon subsequent cooling. Hot ductility was determined by the reduction of area, not by elongation to rupture. In most cases, the *ZST* values are determined virtually identically to the values of nil ductility temperature *NDT* (°C) and embody the temperature at which dendritic solid phases are connected with each other and plastic deformation can start after a considerable progress of solidification (with approximately 10% of residual liquid). In contrast, the *NST* value determined by the much simpler methodology described above is not associated with any partial or full melting of the specimen during heating. In addition, this *NST* value is always higher than the *NDT* value (according to the authors of the paper [5,6,11] on average by 35 °C with a tolerance of ± 20 °C).

Support for these claims can be found in Figure 7 which graphically compares the *ZST* or *NST* values determined by various authors. Only the indisputable *ZST* values were located by digitizing the previously published graphs [39–42]. In this case, T_S value corresponds to the equilibrium solidus temperature in the Fe-C binary diagram and thus does not reflect the influences of other chemical elements. This was reflected in the less accurate linear dependence $NST = f(T_S)$—compare in Figure 6. The values of *ZST* determined by using of IDS software and the values of *ZST* determined in [40] were practically the same. All datasets exhibits a linear dependency, but with different slopes and intercepts. The key is that for comparable carbon and solidus temperatures, relationship $ZST > NST$ is valid. Therefore, the values *ZST* and *NST* must be considered to be fundamentally dissimilar, which is mainly due to the different methodology of their determination. Moreover, these material characteristics may be affected by the rate of temperature change during the test [43].

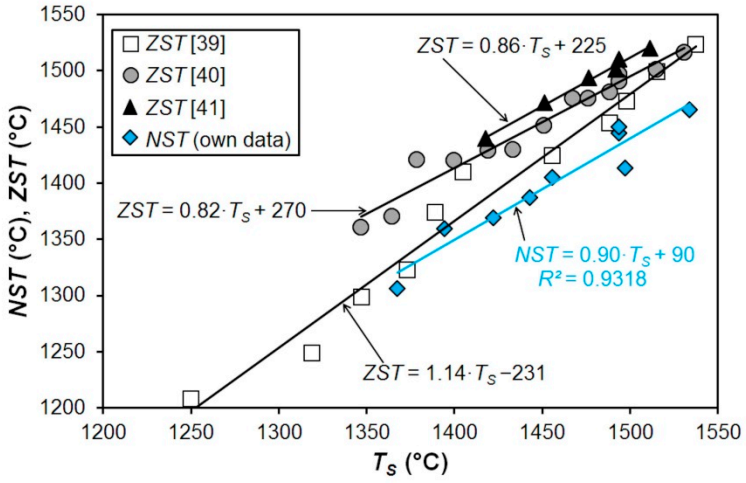

Figure 7. Zero strength temperature and measured nil-strength temperature values depending on the equilibrium solidus temperature.

4. Conclusions

With the use of physical tests performed on the universal plastometer Gleeble 3800 and calculations in the IDS software, the nil-strength temperatures, zero strength temperatures and solidus temperatures

of nine non-alloy carbon steels were determined. Apart from that, solidus temperatures were also calculated with the use of four equations expressing a mathematical relation of this temperature to the chemical composition of the investigated steels.

The nil-strength temperature and zero strength temperature declined with increasing carbon content in the investigated steels. The zero strength temperatures determined by calculation in the IDS software during solidification were approximately about 43–85 °C higher than the nil-strength temperatures determined experimentally during heating of the investigated steels.

The presented equations designed for the calculation of the solidus temperature bring forth a relatively quick and easy approach to gaining the results, but it is not possible to use all of them for the wide range of the chemical compositions of the investigated steels. The solidus temperatures obtained using Equations (2) and (3) or by calculation in the IDS software declined with increasing carbon content in the investigated steels, which corresponds to the Fe-Fe_3C diagram. The differences between the solidus temperatures calculated in the IDS software and with the use of Equations (2) and (3) were not higher than 50 °C.

The increased content of sulfur in the free-cutting steel B always resulted in a decline of the solidus temperatures determined by calculation. This fact was also found out in the case of the determined nil-strength and zero strength temperatures.

The main findings were as follows:

- It is clear from the obtained results that the nil-strength temperature determined during heating is not the same value as the zero strength temperature determined during the solidification of steels during their casting.
- The linear dependence of experimentally measured nil-strength temperature on the calculated zero strength temperature of the investigated steels was determined.
- The mathematical relations which described with high accuracy a linear dependence of the nil-strength and zero strength temperatures of the investigated steels on the solidus temperature were determined. Equations (9) and (10), together with Equation (2), enable a relatively easy and accurate prediction of the nil-strength and zero strength temperatures of carbon steels (during their heating or solidification) in dependence on their chemical composition.
- The obtained results can be applied to optimization processes for the welding, casting or forming of non-alloy carbon steels.

Author Contributions: Conceptualization, P.K. and I.S.; methodology, P.K., B.S., J.M. and A.M.; software, B.S. and Ľ.D.; validation, P.K., I.S. and A.M.; formal analysis, P.K., R.K. and S.R.; investigation, P.K., P.O. and A.M.; resources, J.M. and R.K.; data curation, P.K. and I.S.; writing—original draft preparation, P.K. and I.S.; visualization, P.K., I.S. and A.M.; supervision, P.K.; writing—review and editing, P.K., P.O. and B.S. All authors have read and agreed to the published version of the manuscript.

Funding: The article was created thanks to the project number CZ.02.1.01/0.0/0.0/17_049/0008399 from the EU and CR financial funds provided by the Operational Programme Research, Development and Education, Call 02_17_049 Long-Term Intersectoral Cooperation for ITI, Managing Authority: Czech Republic—Ministry of Education, Youth and Sports, and with the students' grant project SP2020/88 supported at the VSB–Technical University of Ostrava, by the Ministry of Education, Youth and Sports of the Czech Republic.

Conflicts of Interest: The authors declare no conflict of interest. The funders had no role in the design of the study; in the collection, analyses, or interpretation of data; in the writing of the manuscript; or in the decision to publish the results.

References

1. Gryc, K.; Smetana, B.; Žaludová, M.; Michalek, K.; Klus, P.; Tkadlečková, M.; Socha, L.; Dobrovská, J.; Machovčák, P.; Válek, L.; et al. Determination of the Solidus and Liquidus Temperatures of the Real-steel Grades with Dynamic Thermal-analysis Methods. *Mater. Technol.* **2013**, *47*, 569–575.
2. Zhuang, C.L.; Liu, J.H.; Bernhard, C.; Presoly, P. Analysis of Solidification of High Manganese Steels Using Improved Differential Thermal Analysis Method. *J. Iron Steel Res. Int.* **2015**, *22*, 709–714. [CrossRef]

3. Štětina, J. Dynamický model teplotního pole plynule odlévané bramy. Ph.D. Thesis, VSB-TU Ostrava, Ostrava, Czech Republic, 2007. (In Czech).
4. Thomas, B.G.; Samarasekera, I.V.; Brimacombe, J.K. Mathematical Model of the Thermal Processing of Steel Ingots 1. Heat Flow Model. *Metall. Trans. B* **1987**, *18*, 119–130. [CrossRef]
5. Kuzsella, L.; Lukács, J.; Szücs, K. Nil-strength Temperature and Hot Tensile Tests on S960QL High-strength Low-alloy Steel. *Prod. Process. Syst.* **2013**, *6*, 67–78.
6. Mandziej, S.T. Physical Simulation of Metallurgical Processes. *Mater. Technol.* **2010**, *44*, 105–119.
7. Gryc, K.; Smetana, B.; Žaludová, M.; Klus, P.; Michálek, K.; Tkadlečková, M.; Dobrovská, J.; Socha, L.; Chmiel, B. High-temperature Thermal Analysis of Specific Steel Grades. In Proceedings of the 21st International Conference on Metallurgy and Materials Metal 2012, Brno, Czech Republic, 23–25 May 2012; pp. 103–108.
8. Piekarski, B. The influence of Nb, Ti, and Si additions on the liquidus and solidus temperatures and primary microstructure refinement in 0.3C-30Ni-18Cr cast steel. *Mater. Charact.* **2010**, *61*, 899–906. [CrossRef]
9. Khosravifard, A.; Hematiyan, M.R.; Wrobel, L.C. Simultaneous control of solidus and liquidus lines in alloy solidification. *Eng. Anal. Bound. Elem.* **2013**, *34*, 211–224. [CrossRef]
10. Fu, J.W.; Qiu, W.X.; Nie, Q.Q.; Wu, Y.C. Precipitation of TiN during solidification of AISI 439 stainless steel. *J. Alloys Compd.* **2017**, *699*, 938–946. [CrossRef]
11. Sawicki, S.; Dyja, H.; Kawalek, A.; Knapinksi, M.; Kwapisz, M.; Laber, K. High-Temperature Characteristics of 20MnB4 and 30MnB4 Micro-Addition Cold Upsetting Steels and C45 and C70 High-Carbon-Steels. *Metalurgija* **2016**, *55*, 643–646.
12. Böllinghaus, T.; Herold, H. *Hot Cracking Phenomena in Welds*, 1st ed.; Springer: Berlin/Heidelberg, Deutschland, 2005; p. 394.
13. Lukács, J.; Kuzsella, L.; Koncsik, Z.; Gáspár, M.; Meilinger, Á. Role of the Physical Simulation for the Estimation of the Weldability of High Strength Steels and Aluminum Alloys. *Mater. Sci. Forum* **2014**, *812*, 149–154. [CrossRef]
14. Santillana, B.; Boom, R.; Eskin, D.; Mizukami, H.; Hanao, M.; Kawamoto, M. High-Temperature Mechanical Behavior and Fracture Analysis of a Low-Carbon Steel Related to Cracking. *Metall. Mater. Trans. A* **2012**, *43A*, 5048–5057. [CrossRef]
15. Lyczkowska, K.; Adamiec, J.; Jachym, R.; Kwiecinski, K. Properties of the Inconel 713 Alloy Within the High Temperature Brittleness Range. *Arch. Foundry Eng.* **2017**, *17*, 103–108. [CrossRef]
16. Eskin, D.G.; Suyitno; Katgeman, L. Mechanical properties in the semi-solid state and hot tearing of aluminium alloys. *Prog. Mater. Sci.* **2004**, *49*, 629–711. [CrossRef]
17. Andersson, J.; Sjöberg, G.; Chaturvedi, M. Hot Ductility Study of Haynes 282 Superalloy. In Proceedings of the 7th International Symposium on Superalloy 718 and Derivatives, Pittsburgh, PA, USA, 10–13 October 2010. [CrossRef]
18. Smetana, B.; Zla, S.; Kawuloková, M.; Gryc, K.; Strouhalová, M.; Kalup, A.; Tkadlečková, M.; Dobrovská, J.; Michalek, K.; Jonšta, P.; et al. Temperatures of Solidus and Liquidus of Tool Steel. In Proceedings of the 25th Anniversary International Conference on Metallurgy and Materials Metal 2016, Brno, Czech Republic, 25–27 May 2016; pp. 91–96.
19. Kawuloková, M.; Zlá, S.; Dobrovská, J.; Smetana, B.; Kalup, A.; Strouhalová, M.; Vontorová, J.; Válek, L.; Rosypalová, S.; Francová, H. Phase Transformations Temperatures of Real Steel Grade. In Proceedings of the 24th International Conference on Metallurgy and Materials Metal 2015, Brno, Czech Republic, 3–5 June 2015; pp. 636–641.
20. Kawulok, R.; Schindler, I.; Kawulok, P.; Rusz, S.; Opěla, P.; Solowski, Z.; Čmiel, K.M. Effect of Deformation on the Continuous Cooling Transformation CCT Diagram of Steel 32CrB4. *Metalurgija* **2015**, *54*, 473–476.
21. Kawuloková, M.; Smetana, B.; Zlá, S.; Kalup, A.; Mazancová, E.; Váňová, P.; Kawulok, P.; Dobrovská, J.; Rosypalová, S. Study of Equilibrium and Nonequilibrium Phase Transformations Temperatures of Steel by Thermal Analysis Methods. *J. Therm. Anal. Calorim.* **2017**, *127*, 423–429. [CrossRef]
22. Saunders, N.; Guo, Z.; Li, X.; Miodownik, A.P.; Schille, J.P. Using JMatPro to Model Materials Properties and Behavior. *JOM* **2003**, *55*, 60–65. [CrossRef]
23. Andersson, J.O.; Helander, T.; Hoglund, L.H.; Shi, P.F.; Sundman, B. THERMO-CALC & DICTRA, computational tools for materials science. *CALPHAD: Comput. Coupling Phase Diagrams Thermochem.* **2002**, *26*, 273–312. [CrossRef]

24. Diederichs, R.; Bleck, W. Modelling of manganese sulphide formation during solidification. Part I: Description of MnS formation parameters. *Steel Res. Int.* **2006**, *77*, 202–209. [CrossRef]
25. Takeuchi, E.; Brimacombe, J.K. Effect of Oscillation-Mark Formation on the Surface Quality of Continuously Cast Steel Slabs. *Metall. Trans. B* **1985**, *16*, 605–625. [CrossRef]
26. Peitsch, P.R.; Danón, C.A. Comparative Study of 9% Cr Martensitic-ferritic Steels Using Differential Scanning Calorimetry. *Procedia Mater. Sci.* **2015**, *9*, 514–522. [CrossRef]
27. Fabrichnaya, O.; Ullrich, C.; Wendler, M.; Savinykh, G.; Rafaja, D. High-temperature phase transformations in strongly metastable austenitic-martensitic CrMnNi-N-C cast steels. *J. Alloys Compd.* **2016**, *686*, 511–521. [CrossRef]
28. Hechu, K.; Slater, C.; Santillana, B.; Clark, S.; Sridhar, S. A novel approach for interpreting the solidification behaviour of peritectic steels by combining CSLM and DSC. *Mater. Charact.* **2017**, *133*, 25–32. [CrossRef]
29. Gumienny, G. Carbidic Bainitic and Ausferritic Ductile Cast Iron. *Arch. Metall. Mater.* **2013**, *58*, 1053–1058. [CrossRef]
30. Rapiejko, C.; Pisarek, B.; Czekaj, E.; Pacyniak, T. Analysis of AM60 and AZ91 alloy crystallisation in ceramic moulds by thermal derivative analysis (TDA). *Arch. Metall. Mater.* **2014**, *59*, 1449–1455. [CrossRef]
31. Fujimura, T.; Takeshita, K.; Suzuki, R.O. Mathematical analysis of the solidification behavior of multi-component alloy steel based on the heat- and solute-transfer equations in the liquid–solid zone. *Int. J. Heat Mass Tran.* **2019**, *130*, 797–812. [CrossRef]
32. Won, Y.M.; Thomas, B.G. Simple Model of Microsegregation during Solidification of Steels. *Metall. Mater. Trans. A* **2001**, *32A*, 1755–1767. [CrossRef]
33. Kawulok, P.; Schindler, I.; Kawulok, R.; Rusz, S.; Opěla, P.; Kliber, J.; Kawuloková, M.; Solowski, Z.; Čmiel, K.M. Plastometric Study of Hot Formability of Hypereutectoid C–Mn–Cr–V Steel. *Metalurgija* **2016**, *55*, 365–368.
34. Mittinen, J. *Solidification Analysis Package for Steels—User's Manual of DOS Version*, 1st ed.; University of Technology: Helsinky, Finland, 1999.
35. Miettinen, J.; Louhenkilpi, S. Calculation of thermophysical properties of carbon and low-alloyed steels for modeling of solidification processes. *Metall. Mater. Trans. B* **1994**, *25*, 909–916. [CrossRef]
36. Miettinen, J.; Louhenkilpi, S.; Kytonen, H.; Laine, J. IDS: Thermodynamic-kinetic-empirical tool for modelling of solidification, microstructure and material properties. *Math. Comput. Simulat.* **2010**, *80*, 1536–1550. [CrossRef]
37. Adamiec, J.; Kalka, M. Brittleness temperature range of Fe-Al alloy. *JAMME* **2006**, *18*, 43–46.
38. Žídek, M. *Metallurgical Formability of Steels at hot and cold Conditions*, 1st ed.; Aleko: Praha, Czech Republic, 1995. (In Czech)
39. Suzuki, H.G.; Nishimura, S.; Nakamura, Y. Improvement of hot ductility of continuously cast carbon steels. *Trans. ISIJ* **1984**, *24*, 54–59. [CrossRef]
40. Schmidtmann, E.; Rakoski, F. Einfluß des Kohlenstoffgehaltes von 0,015 bis 1 % und der Gefügestruktur auf das Hochtemperaturfestigkeits- und -zähigkeitsverhalten von Baustählen nach der Erstarrung aus der Schmelze (Influence of sulphur and manganese and of the cooling conditions on the structure and toughness properties of structural steels after solidification from the melt). *Arch. Eisenhüttenwes.* **1983**, *54*, 357–362. (In German)
41. Shin, G.; Kajitani, T.; Suzuki, T.; Umeda, T. Mechanical properties of carbon steels during solidification. *Tetsu-to-Hagane* **1992**, *78*, 587–593. [CrossRef]
42. You, D.; Bernhard, C.H.; Wieser, G.; Michelic, S. Microsegregation model with local equilibrium partition coefficients during solidification of steels. *Steel Res. Int.* **2016**, *87*, 840–849. [CrossRef]
43. Flesh, R.; Bleck, W. Crack susceptibility of medium and high alloyed tool steels under continuous casting conditions. *Steel Res.* **1998**, *69*, 292–299. [CrossRef]